# Polarization-independent and omnidirectional nearly perfect absorber with ultra-thin 2D subwavelength metal grating in the visible region

**Wenchao Zhou,[1] Kaiwei Li,[1] Chao Song,[1,2] Peng Hao,[1] Mingbo Chi,[1] Muxin Yu,[1,2] and Yihui Wu[1*]**

[1]*State Key Laboratory of Applied Optics, Changchun Institute of Optics, Fine Mechanics and Physics, Chinese Academy of Sciences, Changchun 130033, China*
[2]*University of Chinese Academy of Sciences, Beijing 100039, China*
[*]*yihuiwu@ciomp.ac.cn*

**Abstract:** A polarization-independent and omnidirectional nearly perfect absorber in the visible region has been proposed. The absorber is two-layer structure consisting of a subwavelength metal grating layer embedded in the high refractive index and lossless dielectric layer on the metal substrate. Extraordinary optical absorption with absorption peaks of over 99% can be achieved over the whole visible region for both TM and TE polarization. This absorption is attributed to cavity mode (CM) resonance caused by the coupled surface plasmon polaritons (SPP). Through adjusting the grating thickness, the absorption peak can be tuned linearly, which is highly advantageous to design various absorbers. Furthermore, the absorbance retains ultra-high over a wide angular range of incidence for both TM and TE polarization. This nearly perfect absorber offers great potential in the refractive index (RI) sensors, integrated photodetectors, solar cells and so on.



**OCIS codes:** (310.6628) Subwavelength structures, nanostructures; (050.0050) Diffraction and gratings; (240.6680) Surface plasmons; (300.1030) Absorption.

## References and links

1. R. A. Pala, J. White, E. Barnard, J. Liu, and M. L. Brongersma, "Design of plasmonic thin-film solar cells with broadband absorption enhancements," Adv. Mater. **21**(34), 3504–3509 (2009).
2. J. J. Talghader, A. S. Gawarikar, and R. P. Shea, "Spectral selectivity in infrared thermal detection," Light Sci.Appl. **1**(8), e24 (2012).
3. M. L. Brongersma, Y. Cui, and S. Fan, "Light management for photovoltaics using high-index nanostructures," Nat. Mater. **13**(5), 451–460 (2014).
4. C. F. Guo, T. Sun, F. Cao, Q. Liu, and Z. Ren, "Metallic nanostructures for light trapping in energy-harvesting devices," Light Sci.Appl. **3**(4), e161 (2014).
5. C. Hu, Z. Zhao, X. Chen, and X. Luo, "Realizing near-perfect absorption at visible frequencies," Opt. Express **17**(13), 11039–11044 (2009).
6. J. N. Munday and H. A. Atwater, "Large integrated absorption enhancement in plasmonic solar cells by combining metallic gratings and antireflection coatings," Nano Lett. **11**(6), 2195–2201 (2011).
7. E. Battal, T. A. Yogurt, L. E. Aygun, and A. K. Okyay, "Triangular metallic gratings for large absorption enhancement in thin film Si solar cells," Opt. Express **20**(9), 9458–9464 (2012).
8. Z. Fang, Y. R. Zhen, L. Fan, X. Zhu, and P. Nordlander, "Tunable wide-angle plasmonic perfect absorber at visible frequencies," Phys. Rev. B **85**(24), 245401 (2012).
9. N. I. Landy, S. Sajuyigbe, J. J. Mock, D. R. Smith, and W. J. Padilla, "Perfect metamaterial absorber," Phys. Rev. Lett. **100**(20), 207402 (2008).
10. N. Liu, M. Mesch, T. Weiss, M. Hentschel, and H. Giessen, "Infrared perfect absorber and its application as plasmonic sensor," Nano Lett. **10**(7), 2342–2348 (2010).
11. Y. Cui, K. H. Fung, J. Xu, H. Ma, Y. Jin, S. He, and N. X. Fang, "Ultrabroadband light absorption by a sawtooth anisotropic metamaterial slab," Nano Lett. **12**(3), 1443–1447 (2012).
12. X. Liu, T. Starr, A. F. Starr, and W. J. Padilla, "Infrared spatial and frequency selective metamaterial with near-unity absorbance," Phys. Rev. Lett. **104**(20), 207403 (2010).
13. X. Shen, T. J. Cui, J. Zhao, H. F. Ma, W. X. Jiang, and H. Li, "Polarization-independent wide-angle triple-band metamaterial absorber," Opt. Express **19**(10), 9401–9407 (2011).

14. X. Xiong, S. C. Jiang, Y. H. Hu, R. W. Peng, and M. Wang, “Structured metal film as a perfect absorber,” Adv. Mater. **25**(29), 3994–4000 (2013).
15. J. Le Perchec, P. Quémerais, A. Barbara, and T. López-Ríos, “Why metallic surfaces with grooves a few nanometers deep and wide may strongly absorb visible light,” Phys. Rev. Lett. **100**(6), 066408 (2008).
16. F. Pardo, P. Bouchon, R. Haïdar, and J. L. Pelouard, “Light funneling mechanism explained by magnetoelectric interference,” Phys. Rev. Lett. **107**(9), 093902 (2011).
17. A. Polyakov, K. F. Thompson, S. D. Dhuey, D. L. Olynick, S. Cabrini, P. J. Schuck, and H. A. Padmore, “Plasmon resonance tuning in metallic nanocavities,” Sci Rep **2**, 933 (2012).
18. K. Aydin, V. E. Ferry, R. M. Briggs, and H. A. Atwater, “Broadband polarization-independent resonant light absorption using ultrathin plasmonic super absorbers,” Nat. Commun. **2**, 517 (2011).
19. S. Butun and K. Aydin, “Structurally tunable resonant absorption bands in ultrathin broadband plasmonic absorbers,” Opt. Express **22**(16), 19457–19468 (2014).
20. N. I. Zheludev and Y. S. Kivshar, “From metamaterials to metadevices,” Nat. Mater. **11**(11), 917–924 (2012).
21. W. Zhou, Y. Wu, M. Yu, P. Hao, G. Liu, and K. Li, “Extraordinary optical absorption based on guided-mode resonance,” Opt. Lett. **38**(24), 5393–5396 (2013).
22. T. Cao, C. W. Wei, R. E. Simpson, L. Zhang, and M. J. Cryan, “Broadband polarization-independent perfect absorber using a phase-change metamaterial at visible frequencies,” Sci Rep **4**, 3955 (2014).
23. S. I. Bozhevolnyi and J. Jung, “Scaling for gap plasmon based waveguides,” Opt. Express **16**(4), 2676–2684 (2008).
24. S. Collin, F. Pardo, and J. L. Pelouard, “Waveguiding in nanoscale metallic apertures,” Opt. Express **15**(7), 4310–4320 (2007).
25. P. Bouchon, F. Pardo, B. Portier, L. Ferlazzo, P. Ghenuche, G. Dagher, C. Dupuis, N. Bardou, R. Haidar, and J. L. Pelouard, “Total funneling of light in high aspect ratio plasmonic nanoresonators,” Appl. Phys. Lett. **98**(19), 191109 (2011).
26. H. T. Miyazaki and Y. Kurokawa, “Controlled plasmon resonance in closed metal/insulator/metal nanocavities,” Appl. Phys. Lett. **89**(21), 211126 (2006).
27. M. G. Moharam and T. K. Gaylord, “Rigorous coupled-wave analysis of metallic surface-relief gratings,” J. Opt. Soc. Am. A **3**(11), 1780–1787 (1986).
28. S. Peng and G. M. Morris, “Efficient implementation of rigorous coupled-wave analysis for surface-relief gratings,” J. Opt. Soc. Am. A **12**(5), 1087–1096 (1995).
29. A. D. Rakic, A. B. Djurisic, J. M. Elazar, and M. L. Majewski, “Optical properties of metallic films for vertical-cavity optoelectronic devices,” Appl. Opt. **37**(22), 5271–5283 (1998).
30. J. S. White, G. Veronis, Z. Yu, E. S. Barnard, A. Chandran, S. Fan, and M. L. Brongersma, “Extraordinary optical absorption through subwavelength slits,” Opt. Lett. **34**(5), 686–688 (2009).
31. S. H. Chang and Y. L. Su, “Mapping of transmission spectrum between plasmonic and nonplasmonic single slit. I:resonant transmission,” J. Opt. Soc. Am. B **32**(1), 38–44 (2015).
32. K. M. Mayer and J. H. Hafner, “Localized surface plasmon resonance sensors,” Chem. Rev. **111**(6), 3828–3857 (2011).

## 1. Introduction

In last decade, extraordinary optical absorption in nanostructures has attracted much attention because of its potential applications in photodetectors and photovoltaics [1–4]. A tremendous number of structures have been proposed, such as plasmonic nanostructures [5–8] and metamaterial absorbers [9–14]. Among these structures, metamaterial absorbers have attracted considerable interest due to their unique electromagnetic properties, such as the feasibility of arbitrary effective permittivity and permeability originating from the electromagnetic resonance inside the metamaterial structures [9]. The metal-insulator-metal (MIM) structure and deep subwavelength rectangular-shaped groove are the most frequently investigated configurations of the metamaterial absorbers [10, 15–19]. However, perfect impedance matching needs tighter fabrication tolerances to obtain an absorption peak that is very sensitive to geometrical adjustment [9]. In addition, to display the metamaterial behavior, the structural units usually are much smaller than the wavelength of the incident radiation [20], which hiders the development of these absorbers limited by the current nanofabrication technology.

Recently, we have presented a novel absorption structure based on guided-mode resonance [21]. The absorption efficiency can be optimized up to 99.16%.Though this type of absorber has good fabrication tolerances against the fill factor, the structure is sensitive to the incidence angle due to the existence of guided resonance. In this paper, we propose another polarization-independent, omnidirectional and nearly perfect absorber in the visible region. Although the other absorbers using a phase-changing metamaterial (PCM) can also achieve nearly perfect absorption, the application of PCMs depends upon the crystallization rate of the material [22]. This novel absorber is composed of two-dimensional (2D) subwavelength metallic grating surrounded by a high refractive index and lossless dielectric layer deposited on the metal substrate. Usually, the effective refractive index increases as the slit width becomes narrow [23, 24]. Thus, in order to decrease the grating thickness, high aspect ratio nanostructures are always required. Different from the previous reports [15–17, 25, 26], a high refractive material is filled in the grating to reduce the grating height by increasing the effective refractive index. This absorption is attributed to the cavity mode behaving like gap surface plasmon mode in the slits of the grating. Besides, this absorber can be utilized as a plasmonic sensor for refractive sensor with sensitivity of around 300nm/RIU.

## 2. Structure design and simulations

Figure 1(a) illustrates the proposed structure consisting of a subwavelength metal grating embedded in the $Si_3N_4$ layer and the metal substrate. The substrate and the grating material is aluminum (Al). Because of the presence of the metal substrate, the transmission of this structure is totally eliminated, i.e., the transmittance equals to 0. This structure is characterized by the grating period P, fill factor f, grating thickness d (equal to the $Si_3N_4$ layer thickness), groove width w, the substrate thickness h. The 2D periodic gratings have the same geometric parameters in the x and y directions, since the geometric symmetry is essential to realize the polarization independence. We perform the simulation by utilizing rigorous coupled wave analysis (RCWA) method [27, 28]. In all numerical simulations, aluminum is estimated by the Lorentz-Drude model taking into account interband transitions [29]. And we fixed the refraction index of $Si_3N_4$ as 2.0. The substrate thickness is set to be 100nm. The normal TM light with its magnetic field polarized normal to the incident plane (y direction) is illuminated in the simulations at first when the non-angle parameters, such as fill factor, period and so on, are analyzed. Then we will simulate the effect of the incident angle on the absorption spectra. Finally, the properties of this absorber as a RI sensor are investigated.

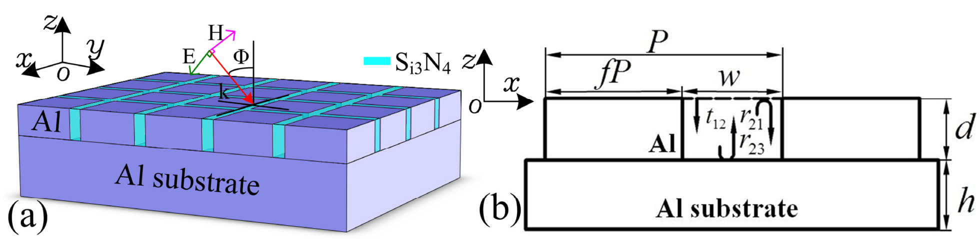


Fig. 1. (a) Schematic of the proposed absorber with a 2D subwavelength metal grating embedded in the lossless and high refractive dielectric layer atop the metal substrate. (b) Front view showing the structural parameters and the relevant scattering coefficients.

We argue that the nearly perfect absorption originated from the cavity mode supported inside the slits, which acts as a truncated metal-insulator-metal plasmon waveguide as shown in Fig. 1(b). Truncation of such a waveguide results in strong reflections at the slits terminations, and a resonant cavity can be subsequently formed. In this cavity, the incident light can excite the cavity mode with a transmission coefficient $t_{12}$. At the same time, at the top and bottom interfaces, the propagating plasmon experiences multiple reflections, with complex reflection coefficients $r_{21}$ and $r_{23}$, respectively, and which include a magnitude and phase. The eigenfrequencies of the CM resonance are determined by the resonant length d, and given by the formula [30]:

$$\phi_{21} + \phi_{23} + 2k_{MIM} d = 2\pi m, \tag{1}$$

where $\phi_{21}$ and $\phi_{23}$ are phases acquired by the CM and caused by the reflection at the two terminations, m is the resonance order integer, and $k_{MIM}$ is the complex wave vector of the plasmon mode in the slits.

#232547 - $15.00 USD Received 15 Jan 2015; revised 12 Mar 2015; accepted 30 Mar 2015; published 7 Apr 2015

## 3. Results and discussion

Figure 2 presents the absorptance along with the reflectance for this absorbing structure at the normal incidence, where the period P = 0.2μm, the thickness of this grating d = 0.035μm and fill factor f = 0.8. The resonant absorption peak is found at λ = 0.540μm, with the absorption efficiency of 0.99836 shown in Fig. 2(a). In order to investigate this optical absorption in this system, we perform the electromagnetic field distributions at the absorption peak, as shown in Fig. 2(b). Nearly all the electromagnetic field can be confined within the grooves due to the cavity mode. A high refractive index $Si_3N_4$ is used to increase the optical effective thickness of the grooves, thus the thin metal can absorb the almost incident power.

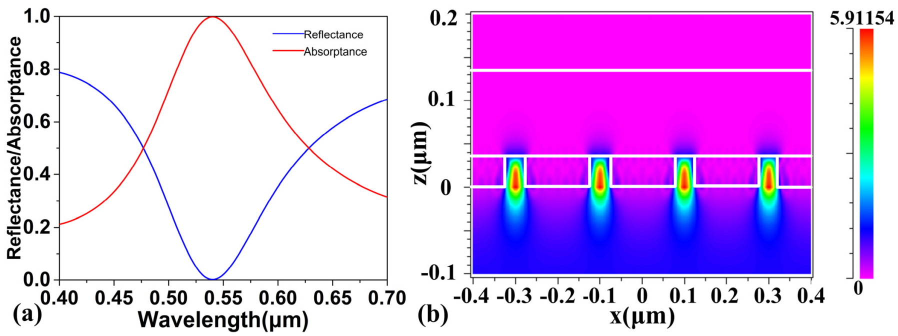


Fig. 2. (a) Absorption spectra of this 2D absorber for the TM polarization. (b) Simulated distributions of the electric field at resonant peak in Fig. 2(a), the white lines in these figures show the configuration.

The dependence of absorption peak on the fill factor and the grating period is demonstrated in Fig. 3. The absorption efficiency of up to 99.9964 can be reached, nearly perfect, in this figure. In general, the resonant wavelength of the metallic slits is determined by three factors: the pure Fabry-Perot (FP) mode, the phase shift at the end faces and the effective refractive index $n_{eff}$ obtained from the MIM waveguide dispersion. The corresponding analytical form of the resonance peak can be expressed as [31]

$$\lambda_{peak} = n_{eff} \times \left[ \frac{2n_0 d}{m} + d \frac{\frac{4w}{md}\left[\ln\left(\frac{\pi m w}{2n_0 d}\right) - \frac{3}{2}\right]}{2\frac{w}{d}\left[\ln\left(\frac{\pi m w}{2n_0 d}\right) - \frac{1}{2}\right] - \pi} \right], \tag{2}$$

The first term on the right side in the Eq. (2) is the FP resonance condition; the second term is the amount of the wavelength red-shift owing to the slit end faces.

The absorption peak blue shifts as the grating period increases and the fill factor decreases due to the slit width w = (1-f)P, which makes the effective index reduce. However, when the fill factor approximates 1, this absorption efficiency decreases dramatically displayed in Fig. 3(a). This phenomenon is in that more and more powers inside the narrow groove are reflected instead of being absorbed. On the other hand, the resonant absorption peak wavelength, on the contrary, red shifts as the period continues increasing. The reason is that the SPP coupling into the MIM plasmon waveguide becomes less significant as the gap width increases. Consequently, the phase-shift effect due to the slit end faces dominates [31]. In addition, the absorption over 99% can be achieved with the width of the slits up to 100nm at the period of 0.5 μm in Fig. 3(b). This is favorable to nanofabrication due to the low aspect ratio.

#232547 - $15.00 USD Received 15 Jan 2015; revised 12 Mar 2015; accepted 30 Mar 2015; published 7 Apr 2015

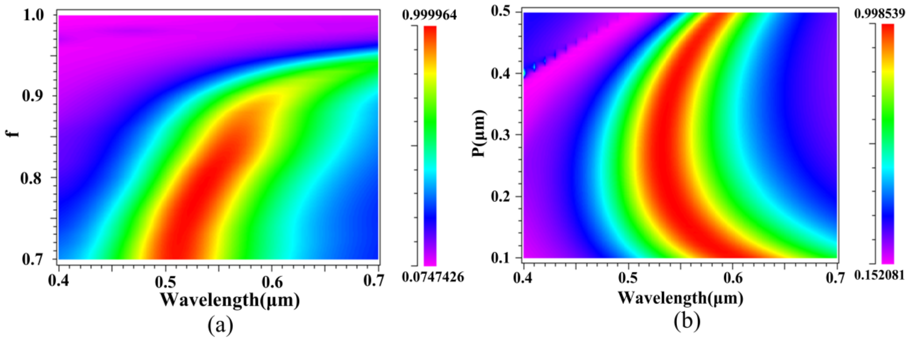


Fig. 3. Absorbance spectra plotted as a function of grating fill factor (a) and period (b), in Fig. (a), P = 0.2μm, d = 0.035μm; in Fig. (b), f = 0.8, d = 0.035μm.

According to Eq. (1), the resonant absorption peak is dependent on the Al grating thickness. Therefore, the peak wavelength can be adjusted readily via this parameter depicted in Fig. 4. From this figure, we found that the absorption peak in visible region can be obtained when the grating thickness ranged from 19nm to 50nm (about λ/20). And the resonant wavelength can be varied approximately linearly with fixed slit width, where the contribution of the phase shift can be ignored compared to the F-P mode. In addition, the absorption above 99% can be obtained in the whole visible region.

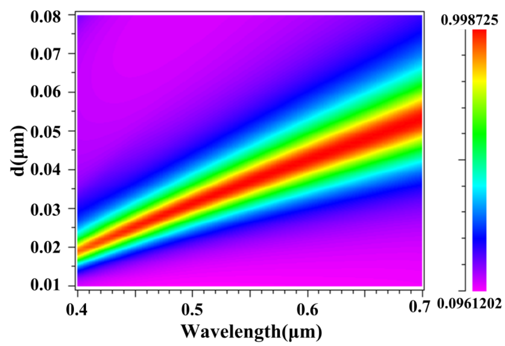


Fig. 4. Absorption spectrum dependence on the thickness of the grating (P = 0.2μm, f = 0.8).

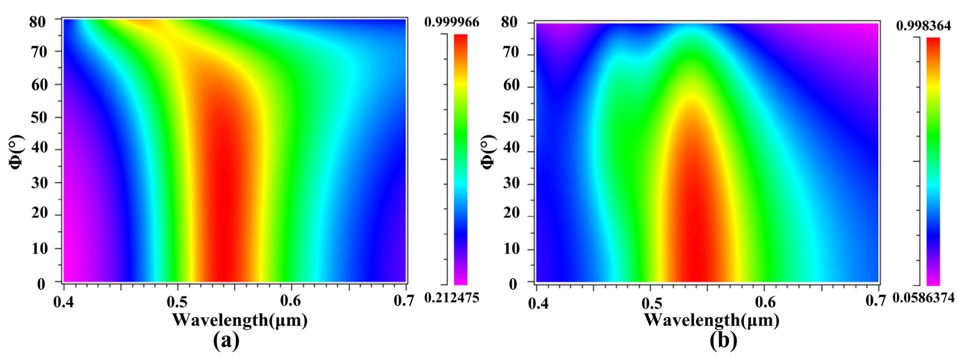


Fig. 5. Absorption spectrum dependence on the incident angle for TM (a) and TE (b) polarizations (P = 0.2μm, f = 0.8, d = 0.035μm).

Because of the inherent characteristic of cavity mode indicated in Eq. (1), the effective thickness of the groove is nearly unchanged with the increasing angle of incidence. Thus, the almost perfect absorptivity of this proposed absorber structure is very robust to the incident angle as shown in Fig. 5. As shown in this figure, the absorption can be observed at large incident angle up to 60° for both TM and TE polarization, which is beneficial to practical application over a wide range of incident angle.

Besides these properties mentioned above, the resonant wavelength also can be determined by the refractive index of the dielectric medium in the slit. When the lossless $Si_3N_4$ layer is replaced by the liquid, we can utilize this absorber as plasmonic sensor for refractive index sensing. Figure 6 shows the simulated reflectance spectra for solutions with different refractive indices. In this structure, the grating period P = 0.2μm, fill factor f = 0.8, grating thickness d = 0.05μm. The grating thickness of the new re-designed absorber increases slightly due to the lower refractive index in order to fix the working wavelength at around 0.5μm. Usually, sensitivity of RI sensor can be defined as the ratio of the change in wavelength to the change in refractive index unit (RIU), $S = \Delta\lambda / \Delta n$ . When the RI ranges from 1.33 to 1.41 in steps of 0.02, we can get different wavelengths: 0.488μm, 0.493μm, 0.499μm, 0.504μm and 0.510μm, respectively. Our simulated results are approximately 300nm/RIU, which is compatible with the current localized surface plasmon resonance (LSPR) sensor [32].

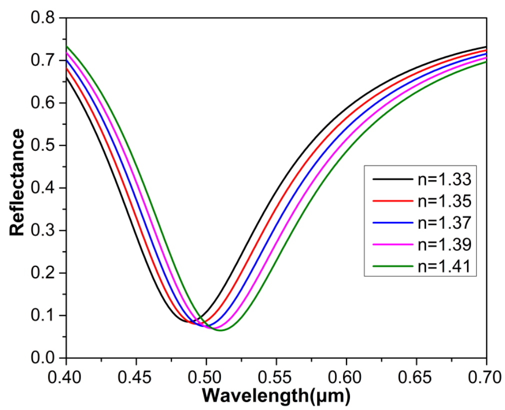


Fig. 6. Simulated reflectance spectra of this absorber sensor for solutions with different refractive indices.

## 4. Conclusions

In conclusion, we have proposed a nearly perfect polarization-independent and omnidirectional absorber with a metal grating embedded in a lossless dielectric layer atop the metal substrate. This absorption is due to the cavity mode cause by the gap plasmon in the groove. The influence of different factors on the absorption is explored in detail. This absorber has an absorption peak with the absorptivity over 99% in the whole visible region. Through tuning the grating thickness from 19nm to 50nm, varied absorption peaks can be obtained. Furthermore, the presented absorber is robust to the incidence angle, which offers great potential in the wide-angle practical application such as solar cells, thermal-photovoltaics, photodetectors etc. Finally, we utilize this absorber as a RI sensor and 300nm/RIU sensitivity can be obtained comparable to the traditional LSPR sensors.

## Acknowledgment

This work is supported by the National High Technology Research and Development Program (No. 2012AA040503) National Key Foundation (No.11034007) and National Science Foundation (No. 61102023) of China, the development plan project of Jilin Province Science and Technology (No. 20120329).